



HAL
open science

Coupling fluid flow, heat transfer and thermal denaturation-aggregation of beta-lactoglobulin using an Eulerian/Lagrangian approach

Etienne E. Chantoiseau, Artemio Plana-Fattori, C. Doursat, D. Flick

► **To cite this version:**

Etienne E. Chantoiseau, Artemio Plana-Fattori, C. Doursat, D. Flick. Coupling fluid flow, heat transfer and thermal denaturation-aggregation of beta-lactoglobulin using an Eulerian/Lagrangian approach. *Journal of Food Engineering*, 2012, 113 (2), pp.234-244. 10.1016/j.jfoodeng.2012.05.043 . hal-00841043

HAL Id: hal-00841043

<https://institut-agro-rennes-angers.hal.science/hal-00841043v1>

Submitted on 16 Dec 2020

HAL is a multi-disciplinary open access archive for the deposit and dissemination of scientific research documents, whether they are published or not. The documents may come from teaching and research institutions in France or abroad, or from public or private research centers.

L'archive ouverte pluridisciplinaire **HAL**, est destinée au dépôt et à la diffusion de documents scientifiques de niveau recherche, publiés ou non, émanant des établissements d'enseignement et de recherche français ou étrangers, des laboratoires publics ou privés.

Accepted Manuscript

Coupling fluid flow, heat transfer and thermal denaturation-aggregation of beta-lactoglobulin using an Eulerian/Lagrangian approach

Etienne Chantoiseau, Artemio Plana-Fattori, Christophe Dousat, Denis Flick

PII: S0260-8774(12)00275-0

DOI: <http://dx.doi.org/10.1016/j.jfoodeng.2012.05.043>

Reference: JFOE 6979

To appear in: *Journal of Food Engineering*

Received Date: 17 August 2011

Revised Date: 3 May 2012

Accepted Date: 27 May 2012

Please cite this article as: Chantoiseau, E., Plana-Fattori, A., Dousat, C., Flick, D., Coupling fluid flow, heat transfer and thermal denaturation-aggregation of beta-lactoglobulin using an Eulerian/Lagrangian approach, *Journal of Food Engineering* (2012), doi: <http://dx.doi.org/10.1016/j.jfoodeng.2012.05.043>

This is a PDF file of an unedited manuscript that has been accepted for publication. As a service to our customers we are providing this early version of the manuscript. The manuscript will undergo copyediting, typesetting, and review of the resulting proof before it is published in its final form. Please note that during the production process errors may be discovered which could affect the content, and all legal disclaimers that apply to the journal pertain.



Title:

Coupling fluid flow, heat transfer and thermal denaturation-aggregation of beta-lactoglobulin using an Eulerian/Lagrangian approach

Authors:

Etienne CHANTOISEAU
Artemio PLANA-FATTORI
Christophe DOUSAT
Denis FLICK

Affiliation (all the authors):

- (1) AgroParisTech, UMR1145 Ingénierie Procédés Aliments, Massy, France
- (2) INRA, UMR1145 Ingénierie Procédés Aliments, Massy, France
- (3) Le Cnam, UMR1145 Ingénierie Procédés Aliments, Massy, France

Corresponding Author Address:

Artemio Plana Fattori
AgroParisTech – MMIP
16 rue Claude Bernard, 75231 Paris CEDEX 5, France
phone: +33.1.44.08.86.84
fax: +33.1.44.08.16.66
e-mail: artemio.planafattori@agroparistech.fr

1 **1. Introduction**

2

3 Thermal processing techniques have been applied to improve quality and
4 safety of food products and to extend their shelf life (Wang and Sun, 2006). In the dairy
5 industry, billions of liters of milk are processed every year for pasteurization or sterilization.
6 Fouling of heat exchangers is an issue because it reduces heat transfer efficiency and
7 increases pressure drop, hence affecting the economy of processing plants. As a result of
8 fouling, there is the possibility of deterioration in the product quality because the process
9 fluid cannot be heated up to the required temperature. Although representing only about 5 %
10 of the milk solids, whey proteins account for more than 50 % of the fouling deposits
11 occurring at temperatures below 110 °C (Bansal and Chen, 2006). The understanding of
12 fouling mechanisms has progressed since the 1970's, which include not only the aggregation
13 of beta-lactoglobulin with other protein molecules but also the influence of aggregates on
14 heat transfer between walls and the process fluid.

15 The structure of whey proteins can be significantly altered depending on the duration
16 and severity of heat treatment. With increasing temperatures whey proteins unfold and can
17 aggregate, either themselves or with other species. Aggregates including whey proteins are
18 relevant to human nutrition (de Wit, 1998) and health (Navarra *et al.*, 2007). Among other
19 applications in the food industry, whey protein aggregates with particle sizes ranging between
20 0.1 and 20 micrometers have been incorporated as successful fat replacers into low-fat stirred
21 yoghurts, because they provide sensory sensations close to those associated with the presence
22 of fat milk (Janhoj *et al.*, 2006). Modeling of whey protein aggregation induced by heat
23 treatment can therefore provide assistance in understanding biophysical processes as well as
24 in designing processing units.

25 This study is devoted to the numerical modeling of the evolution of a suspension of
26 whey proteins under continuous thermal treatment. The beta-lactoglobulin is taken as an
27 example among the whey proteins, and for the sake of simplicity it is taken alone in the
28 suspension. It is the most abundant protein found in the whey fraction of cow milk, and also
29 the dominant whey protein in heat-induced fouling (Bansal and Chen, 2006). Its structure and
30 properties have been studied since the 1930's with the help of different biochemical
31 techniques (Sawyer and Kontopidis, 2000). Denaturation-aggregation of beta-lactoglobulin
32 occurs following different stages: i) the dissociation of native dimers existing under
33 physiological conditions into native monomers, when the temperature increases above 40 °C;
34 ii) the reversible partial unfolding of monomers and the formation of a thermally induced
35 molten globule state when the temperature increases above 60 °C; and iii) depending on
36 operating conditions, the occurrence of irreversible intra-molecular interactions resulting in
37 the formation of aggregates (Tolkach and Kulozik, 2007). An overview about the thermal
38 behavior of the beta-lactoglobulin at temperatures up to 150 °C, including the influence of
39 pH, has been presented by de Wit (2009).

40 Reaction kinetic approaches have been applied for studying the thermal denaturation-
41 aggregation of the beta-lactoglobulin. Such a strategy can provide information related to the
42 main stages of the proteins evolution under heat treatment, namely the concentration of
43 native monomers and that of partially unfolded monomers, and then the aggregates
44 concentration (Tolkach and Kulozik, 2007). Nevertheless, kinetic descriptions cannot provide
45 information regarding the evolution of particle sizes along the process unit. According to
46 Bansal and Chen (2006), efforts remain to be accomplished in assessing the role of different
47 types of aggregates on the fouling deposit formation, as well as in generalizing mitigation
48 strategies. The evolution of particle sizes along the process unit can also be relevant to the
49 sensory and rheological properties of products like yoghurt (Torres *et al.*, 2011).

50 The evolution of a suspension of beta-lactoglobulin under continuous thermal
51 treatment involves the occurrence of fluid flow, heat transfer and product transformation.
52 These processes are coupled: on one hand, the product transformation depends on the
53 operation conditions (velocity, shear and temperature fields); on the other hand, the liquid
54 food thermal and rheological properties are themselves modified as a result of the product
55 transformation. Such a two-way dependence is put in evidence in Figure 1. The suspension
56 flows along a tubular heat exchanger, which is represented by an axially-symmetric
57 rectangular domain; the inlet and outlet are represented by the left and right sides of the
58 domain, and the suspension is heated from the wall (bottom of domain).

59 In Figure 1a, it is assumed that fluid parcels move according to a plug-flow velocity
60 field, and that they are exposed to a temperature field depending only on the distance from
61 the exchanger inlet. Such a one-dimensional (1D) model, neglecting the radial dependence of
62 both velocity and temperature, represents the simplest way to characterize the path to be
63 followed by fluid parcels along a heat exchanger. At the inlet the suspension is assumed to
64 contain monomers only. Upon exposure to heat the temperature of suspension can reach the
65 threshold value for unfolding; after that, unfolded monomers can aggregate. At the outlet, the
66 suspension contains remaining monomers and particles of different sizes resulting from
67 aggregation. In Figure 1a, the resulting particle size distribution is characterized by a
68 qualitative width A .

69 However, as shown in Figure 1b, one cannot neglect the fact that fluid parcels move
70 slower near heating walls. Such fluid parcels undergo dynamical and thermal (and hence
71 kinetic) histories in the process unit that are different from those associated with parcels
72 running far from walls. As a consequence, the extension of unfolding and aggregation
73 depends no longer on the distance from the exchanger inlet only, but on those histories
74 experienced by each fluid parcel. The extension of the product transformation is therefore

75 expected to increase towards the wall. Different size distributions can be obtained at the
76 outlet, depending on the radial position (see Figure 1b); as a result, the bulk size distribution
77 can be broader than that obtained with the 1D model (compare widths A and B). The
78 formation of larger particles allows an increase of the volume associated with the suspension
79 solid fraction, which in turn can modify the suspension viscosity. Figure 1b puts in evidence
80 the role played by dynamical and thermal histories experienced by fluid parcels, showing that
81 both the velocity and the temperature depend on the radial distance. We argue that naive
82 assumptions about fluid flow and heat transfer (like the 1D model, Figure 1a) can provide a
83 biased picture regarding particle sizes at the heat exchanger outlet.

84 In order to realistically represent the denaturation-aggregation of beta-lactoglobulin
85 under thermal treatment, we propose a numerical approach that combines computational fluid
86 dynamics (CFD) for solving the fluid-flow and heat-transfer coupled problem, with a
87 population balance equation (PBE) for evaluating particle aggregation. CFD has become an
88 important tool for research and education in a number of subjects including food science and
89 technology (Norton and Sun, 2006). For instance, CFD has been employed in looking for the
90 optimal design of plate heat exchangers conceived for milk processing (Grijpsperdt *et al.*,
91 2003). The PBE is a common model used to represent the evolution of particulates and
92 dispersed-phase systems when nucleation, growth, aggregation or fragmentation (breakage)
93 of particles occur (Marchisio and Fox, 2005). For instance, the PBE has been adapted in
94 studying the breakage of whey protein precipitates under selected flow conditions (Zumaeta
95 *et al.*, 2007; Bas *et al.*, 2009). Simulation strategies combining CFD and PBE approaches
96 have become feasible with the increase of computation facilities, allowing a more detailed
97 analysis of the particle, droplet or bubble's distribution along the fluid evolution (Marchisio
98 and Fox, 2005; Bhole *et al.*, 2008). In the scope of food science and technology, strategies

99 combining CFD and PBE have been implemented in studying the ice crystallization of
100 sucrose solutions in scraped surface freezers (Lian *et al.*, 2006).

101 In this exploratory study, our aim is to demonstrate that a more realistic representation
102 of the thermal denaturation-aggregation of whey proteins, and particularly of the aggregation
103 of particles under consideration, can be reached with an approach able to take into account
104 the different dynamical and thermal histories associated with fluid parcels in the processing
105 unit. The present approach combines the respective advantages of Eulerian and Lagrangian
106 descriptions of fluid flow, focusing on the coupled representation of fluid flow, heat transfer
107 and whey protein denaturation-aggregation processes. Fluid flow and heat transfer are solved
108 through the finite element method in the Eulerian frame, while the product transformation is
109 evaluated along Lagrangian trajectories associated with representative fluid parcels. Whey
110 protein unfolding is represented by a reaction kinetics of order 1.5, while particle aggregation
111 is assessed after discretization of the PBE. The impact of particle sizes on the suspension
112 viscosity is estimated, allowing the update of the previous solution for fluid flow and heat
113 transfer. The coupled problem is solved by iterating successive Lagrangian and Eulerian steps
114 up to a selected level of convergence.

115 The article is organized as follows. Section 2 presents how the processes of fluid flow,
116 heat transfer, proteins unfolding and particle aggregation are modeled. Section 3 describes
117 how the coupled problem is solved; particular attention is devoted to the solution of the PBE
118 after its discretization, and to the coupling between the PBE solution and CFD results.
119 Section 4 discusses relevant results from our Eulerian-Lagrangian approach, including a
120 comparison with those obtained by neglecting the radial dependence of velocity and
121 temperature fields along the heat exchanger (1D model). Finally, Section 5 provides a
122 summary and indicates future work.

123

124 2. Modeling

125

126 In this study, the suspension of beta-lactoglobulin is represented as a single-phase
127 system. The coupled problem of fluid flow and heat transfer processes is solved on the whole
128 domain using an Eulerian representation while the protein unfolding and particle aggregation
129 are evaluated on a set of fluid parcels whose Lagrangian trajectories depends on the fluid
130 velocity. Such a strategy allows the evaluation of transformation processes that cannot be
131 easily coupled with CFD. This is the particular case of the evaluation of particle aggregation
132 through the PBE approach by employing class or pivot methods, which represent the particle
133 size distribution with the help of a number of size classes.

134

135 2.1. Transformation model

136

137 2.1.1 Case study

138

139 This work deals with the aggregation of beta-lactoglobulin under typical heat treatment. This
140 is achieved by assuming a protein concentration of 3.2 g.L^{-1} , which is a typical value found in
141 cow milk (e.g., Swaisgood, 1995), in water solution at pH 6.8 with 0.1 M NaCl added.
142 Choosing such values ensure that beta-lactoglobulin is under about the same electrochemical
143 environment as in milk. Data for beta-lactoglobulin unfolding and aggregation were obtained
144 for these conditions from experimental work (Aymard et al., 1996; Elofsson et al., 1996; Verheul
145 et al., 1998).

146 In order to test the modeling approach in industrial-like conditions, the coupled fluid flow –
147 heat transfer – transformation model was implemented inside a tubular heat exchanger with
148 length 1 m and radius 5 mm, under a flow rate (10 L.h^{-1}) and a heating rate (10 kW.m^{-2})

149 which lead to a temperature increase from 50 °C (pre-heating temperature) to a maximum
 150 value of about 110 °C. Such a treatment allows a significant level of unfolding-aggregation
 151 and could be achieved on a pilot plant for further comparison with experimental data.

152

153 2.1.2. Protein unfolding

154

155 The denaturation-aggregation of beta-lactoglobulin has been modeled using a reaction
 156 kinetics (Anema and McKenna, 1996). The native protein concentration C_{nat} (mol.m⁻³) at
 157 time t is given by:

158

$$159 \quad \frac{DC_{nat}\{t\}}{Dt} = -k_n C_{nat}^n\{t\} \quad (1)$$

160

161 where n is the reaction order and k_n is the rate constant of the reaction ((mol.m⁻³)⁽¹⁻ⁿ⁾.s⁻¹). The
 162 reaction order n may express the complexity of the unfolding sub-reactions, rather than the
 163 formal order of a classical chemical reaction; in the case of beta-lactoglobulin, it usually
 164 takes values between 1 and 2, commonly 1.5 (Tolkach and Kulozik, 2007). The relationship
 165 between the rate constant and the temperature of the reaction is given by the Arrhenius
 166 equation:

167

$$168 \quad k_n = k_0 \exp\left(-\frac{E_a}{RT}\right) \quad (2)$$

169

170 where k_0 is the frequency factor, E_a the activation energy (J.mol⁻¹), R the universal gas
 171 constant (J.mol⁻¹.K⁻¹) and T the temperature (K).

172 Experimental work on the thermal denaturation-aggregation of the beta-lactoglobulin
173 has put in evidence a marked change in temperature dependence of the reaction rate constant
174 at a threshold of about 85-90 °C (e.g., Lyster, 1970). As a matter of fact, such a behavior
175 results from the occurrence of two regimes: below the temperature threshold, the reaction is
176 limited by the unfolding sub-reactions; above that value, the reaction is limited by the
177 aggregation process (Tolkach and Kulozik, 2007).

178 In this study the thermal denaturation-aggregation of beta-lactoglobulin is represented
179 as a two-step process. Firstly, a reaction kinetics is assumed in estimating the concentration
180 of native proteins which undergo partial reversible unfolding; the temperature is assumed to
181 be the only limiting factor. Secondly, the population balance equation is solved in order to
182 estimate the final concentration of the particles which reach, via aggregation, a number of
183 prescribed sizes. Limiting factors of this second step are the concentration of unfolded
184 proteins, the temperature and the shear rate.

185 A reaction kinetics of order 1.5 is hereafter assumed in representing the thermal
186 unfolding of the beta-lactoglobulin. Table 1 summarizes values of $k_{1.5}$ obtained by Anema
187 and McKenna (1996) for two variants of beta-lactoglobulin under selected temperatures in
188 the range 70-85 °C. Looking for a more representative set of results, an unique Arrhenius
189 equation is assumed to characterize both variants. We estimated the frequency factor and the
190 activation energy by fitting the data presented on Table 1 as a whole:

191

$$192 \quad k_0 = 8.27 \cdot 10^{42} (\text{mol} \cdot \text{m}^{-3})^{(-0.5)} \cdot \text{s}^{-1} \quad (3)$$

193

$$194 \quad E_a = 3.04 \cdot 10^5 \text{ J} \cdot \text{mol}^{-1} \quad (4)$$

195

196 These values are employed into equations (1) and (2) independently on the value assumed by
 197 the temperature as computed by the numerical approach. For temperatures above 85 °C the
 198 extrapolation of the Arrhenius equation can lead to under- or overestimate the unfolding rate,
 199 but unfolding is then no more the limiting factor. Indeed, in our case study, unfolding times
 200 rapidly decrease with the temperature (~1 min at 85 °C, ~1 s at 100 °C); unfolded protein
 201 molecules are immediately engaged in the irreversible aggregation process which becomes
 202 the limiting mechanism.

203

204 2.1.3. Particle aggregation

205

206 Once unfolded, the whey protein monomers are assumed to aggregate according to the
 207 population balance equation proposed by Smoluchowski (1917). This kind of model has been
 208 used for a wide range of applications, including the aggregation of whey proteins (Wu et al.,
 209 2005; Péron et al.; 2007). After assuming no breakage of aggregates, the evolution of the
 210 number of particles containing k monomers (N_k) can be expressed as:

211

$$212 \quad \frac{DN_1\{t\}}{Dt} = k_{1.5} C_{nat}^{1.5}\{t\} N_A - N_1\{t\} \sum_{\ell=1}^M Q_{1,\ell} N_\ell\{t\} \quad (5a)$$

$$213 \quad \frac{DN_k\{t\}}{Dt} = \frac{1}{2} \sum_{\ell=1}^{k-1} Q_{k-\ell,\ell} N_\ell\{t\} N_{k-\ell}\{t\} - N_k\{t\} \sum_{\ell=1}^M Q_{k,\ell} N_\ell\{t\} \quad (5b)$$

214

215 in the cases $k = 1$ and $k > 1$, respectively, where $N_1\{t\}$ is the number of unfolded monomers
 216 at time t , M the maximum number of monomers in an aggregate and N_A the Avogadro
 217 number. The kernel of aggregation $Q_{k,\ell}$ depends on the local temperature, on the continuous

218 phase viscosity (η_w), on the shear rate ($\dot{\gamma}$) (Pa.s), and finally on the radii a_k and a_l of the
 219 aggregates under consideration:

220

$$221 \quad Q_{k,\ell} = \frac{2}{3} \frac{k_B}{W} \frac{T}{\eta_w} \frac{(a_k + a_\ell)^2}{a_k a_\ell} + \frac{4}{3} \frac{\dot{\gamma}}{W} (a_k + a_\ell)^3 \quad (6)$$

222

223 where k_B is the Boltzmann constant and W the Fuchs stability factor. The radius a_k of an
 224 aggregate containing k monomers can be estimated from the monomer radius a_0 and the
 225 aggregates fractal dimension (D):

226

$$227 \quad a_k = a_0 k^{1/D} \quad (7)$$

228

229 The fractal dimension describes the microstructure of the aggregates (Bremer et al., 1989),
 230 allowing to link the number of monomers in an aggregate with its size. This parameter
 231 depends on the monomer / continuous phase couple as well as on the operating conditions
 232 (Byrne et al., 2002).

233 In this exploratory study we focus the attention on the aggregation of beta-
 234 lactoglobulin molecules. Under the considered conditions (pH=6.8 and 0.1 M NaCl), beta-
 235 lactoglobulin monomers exhibit a globular hydrodynamic radius (a_0) of about 2 nm (Aymard
 236 *et al.*, 1996). Under quite similar conditions, comparisons between measurements and
 237 numerical PBE solutions have suggested the value $W=91$ for the Fuchs stability factor
 238 (Elofsson *et al.* 1996). Still under those conditions, the combination of permeability,
 239 rheology, and aggregation kinetics measurements on whey protein gels has indicate the value
 240 $D = 2.4$ for the aggregates fractal dimension (Verheul *et al.*, 1998).

241 Taking into account the concentration of 3.2 g.L^{-1} , the initial suspension contains
 242 $1.0531 \cdot 10^{23}$ monomers per cubic meter. For a maximum total volume fraction of 0.6,
 243 corresponding to the random packing, the largest aggregates should have a radius of about 10
 244 μm and should contain about $M = 10^9$ monomers.

245

246 2.2. Fluid flow and heat transfer models

247

248 2.2.1. Mass, momentum and energy conservation

249

250 The conservation equations for mass, momentum, and energy can be written as:

251

$$252 \nabla \cdot (\rho \mathbf{v}) = 0 \quad (8)$$

253

$$254 \rho (\mathbf{v} \cdot \nabla) \mathbf{v} = \nabla \left(-p \cdot \mathbf{I} + \eta \left(\nabla \mathbf{v} + (\nabla \mathbf{v})^T \right) \right) \quad (9)$$

255

$$256 \rho C_P (\mathbf{v} \cdot \nabla) T = \nabla \cdot (\lambda \nabla T) \quad (10)$$

257

258 Coupled phenomena are illustrated inside a tubular heat exchanger with length 1 m
 259 and radius 5 mm, which is represented through a two-dimension axial-symmetric domain. A
 260 fully developed parabolic flow profile was assumed at the inlet. The flow rate was fixed at 10
 261 liters per hour (mean velocity 0.0351 m.s^{-1}). A uniform flux of 10 kW.m^{-2} is applied on the
 262 heating wall, and the temperature associated with the suspension is assumed to be $50 \text{ }^\circ\text{C}$ at
 263 the inlet. These conditions enable temperatures of about $110 \text{ }^\circ\text{C}$ at the outlet near the heating
 264 wall. Such a temperature enables a relevant degree of protein unfolding and particle

265 aggregation (Tolkach and Kulozik, 2007; de Wit, 2009). According to the Reynolds number,
 266 the flow regime is laminar. Boundary conditions are summarized in Figure 2.

267

268 2.2.2. Suspension viscosity

269

270 The liquid food product under consideration is an aqueous suspension of whey
 271 proteins. The apparent viscosity η associated with the suspension is obtained by multiplying
 272 the continuous phase (pure water) viscosity η_W and the relative viscosity η_R which is a
 273 function of the transformation state. Pure water viscosity depends on the local temperature,
 274 and such an influence can be evaluated through a reference formulation (IAPWS, 2008):

275

$$276 \quad \eta_W = 10^{-6} \left(280.68 \left(\frac{T}{300} \right)^{-1.9} + 511.45 \left(\frac{T}{300} \right)^{-7.7} + 61.131 \left(\frac{T}{300} \right)^{-19.6} + 0.45903 \left(\frac{T}{300} \right)^{-40} \right)$$

277 (11)

278

279 Various approximations have been proposed for estimating the relative viscosity as a
 280 function of the volume fraction (Φ) occupied by the particles under consideration. We have
 281 retained the model proposed by Thomas (1965),

282

$$283 \quad \frac{\eta}{\eta_W} = \eta_R = 1 + 2.5 \Phi + 10.05 \Phi^2 + 0.00273 \exp(16.6 \Phi)$$

283 (12)

284

285 because it provides an increase of relative viscosity with the particle volume fraction which is
 286 intermediate to those obtained with other approximations. The volume fraction is calculated
 287 from the third moment of the aggregates size distribution:

288

$$289 \quad \Phi = \frac{4\pi}{3} \sum_{k=l}^M N_k \{t\} a_k^3 \quad (13)$$

290

291 3. Problem solving

292

293 3.1. Population balance equation resolution

294

295 Once unfolded, the beta-lactoglobulin is subjected to aggregation, represented by the
 296 population balance equation. Its resolution by equation (5) involves the calculation of the
 297 population of a very large number of aggregates size, as an aggregate can contains up to 10^9
 298 monomers. In order to reduce the computational cost, only a limited number of pivots,
 299 indexed by i or j , are here considered. This approach has been used by Batterham et al.
 300 (1981) and Hounslow *et al.* (1988); the latter computed the size distribution of kidney stones
 301 by considering only the particles whose volume is on a regular grid described by $V_{i+1} / V_i = 2$.
 302 This approach can be applied to proteins aggregation by considering the monomers number
 303 of a particle instead of its volume. Here, a monomer number grid is used with $n_{i+1} / n_i = 2$,
 304 where n_i is the number of monomers in the aggregates of pivot i . The aggregates of the pivots
 305 i hence contain $n_i = 2^{i-1}$ monomers. Figure 3 displays an example of population balance and
 306 its repartition on such a pivot grid.

307 As expected, the conservation of quantities such as the total mass or the total number
 308 of particles may be problematic. To solve this issue, (Kumar and Ramkrishna, 1996) showed
 309 that some conditions can lead to the conservation of several quantities using only a reduced
 310 set of pivots.

311 For instance, in the case of the aggregation of particles of size $k = 2$ and $l = 8$ (as
 312 shown on Figure 4), the resulting particle contains 10 monomers and thus, is not among the
 313 calculated pivots. In order to take its presence into account, the number of particles in the two

314 nearest pivots ($k = 8 \Leftrightarrow i = 4$ and $k = 16 \Leftrightarrow j = 5$) are increased by A for pivot i and B for
 315 pivot j . In order to conserve the total number of monomers and of particles in this particular
 316 case, A and B must satisfy:

317 • for the conservation of particles number: $A + B = 1$

318 • for the conservation of monomers number: $A \cdot 8 + B \cdot 16 = 10$

319 This gives $A = 3/4$ and $B = 1/4$ that are the variations on pivots 4 and 5.

320 Regarding the conservation of the total number of monomers and particles on a
 321 geometric grid ($n_{i+1} = 2 n_i$), the proposed solution is equivalent of the earlier proposition of
 322 (Hounslow *et al.*, 1988) that describes the time evolution of the number of particle at the
 323 pivot i , denoted N^i , by:

324

325 for $i = 1$:

326
$$\frac{dN_1\{t\}}{dt} = k_{1.5} C_{nat}^{1.5}\{t\} N_A - N_1\{t\} \sum_{j=1}^M Q_{1,j} N_j\{t\} \quad (14a)$$

327 for $1 < i \leq M$:

328
$$\begin{aligned} \frac{dN_i\{t\}}{dt} = & N_{i-1}\{t\} \sum_{j=1}^{i-2} 2^{j-i+1} Q_{i-1,j} N_j\{t\} + \frac{1}{2} Q_{i-1,i-1} N_{i-1}^2\{t\} - \\ & - N_i\{t\} \sum_{j=1}^{i-1} 2^{j-i} Q_{i,j} N_j\{t\} - N_i\{t\} \sum_{j=i}^M Q_{i,j} N_j\{t\} \end{aligned} \quad (14b)$$

329

330 For the general case of equation 14b, the first term accounts for the creation of aggregates on
 331 the pivot i by aggregation of aggregates from pivot $i-1$ with smaller ones, whereas the second
 332 term accounts for the creation of aggregates on pivots i by aggregation of two aggregates
 333 from pivot $i-1$. The last two terms described the destruction of aggregates on pivot i by
 334 aggregation with either smaller (third term) or larger (last term) aggregates. The number of
 335 pivots is limited to $M = 30$, corresponding to aggregates of radius about 10 μm .

336

337 **3.2. Coupling of fluid flow, heat transfer and product transformation by an Eulerian-** 338 **Lagrangian approach**

339

340 A schematic diagram of the approach is presented in Figure 5. The liquid food is
341 assumed flowing in a tubular heat exchanger, which is represented by a rectangular domain.
342 The dashed red and the bold black lines indicate the axis of symmetry and the heating wall,
343 while the left and right sides represent the domain inlet and outlet respectively. Fluid parcels
344 running nearer to the heating wall move slower than those at the axis; therefore dynamical
345 and thermal histories differ accordingly, leading to different transformation state evolution
346 along their trajectories.

347 The present study combines the respective advantages of Eulerian and Lagrangian
348 descriptions of fluid flow. Fluid flow and heat transfer are solved through the finite element
349 method in the Eulerian frame, while the product transformation is evaluated along
350 Lagrangian trajectories associated with representative fluid parcels.

351 Before the first iteration, a preliminary modeling of fluid flow and heat transfer is
352 needed. It provides a first estimate of the velocity, shear rate and temperature fields along the
353 Eulerian frame. Because this modeling step is performed before any product transformation,
354 the viscosity is here assumed to be the one of the continuous phase (pure water). Eulerian
355 modeling of fluid flow and heat transfer is solved by using a mesh constituted of 100
356 rectangles along the domain's radius and 2000 rectangles along the length.

357 The first step of a given iteration is the estimation of Lagrangian trajectories
358 associated with a number of representative fluid parcels. Each trajectory is defined by a
359 number of positions, and each of them is associated with a given time since the fluid parcel
360 release at the domain inlet. The estimation of trajectory positions from the Eulerian velocity

361 field is performed with the help of a routine implementing a fourth-order Runge-Kutta
362 method (Abramowitz and Stegun, 1972). After a number of sensitivity tests, we found
363 satisfactory the application of 200 trajectories with about 200 positions on each.

364 In the second step, Lagrangian trajectories are employed in the reconstruction of
365 dynamical and thermal histories along the domain. Each history is described by a series of
366 positions, times, and the values associated with the shear rate and temperature. These values
367 are estimated from the last available Eulerian respective fields.

368 Next, the shear rate and temperature histories are employed, along every trajectory, in
369 evaluating the protein unfolding degree (eqs. 1 and 2) and in solving the PBE (eqs. 6 and 14).
370 This is the key step regarding the flexibility of the Eulerian-Lagrangian approach proposed:
371 any available methodology can be employed in evaluating the degree of transformation of the
372 liquid food product along the process unit. The availability of the particle size distribution
373 enables the evaluation of the volume fraction associated with the solid fraction (eq. 13),
374 which is then used for estimating the suspension viscosity (eq. 12).

375 Updated suspension viscosity values have to be informed to the Eulerian model, as a
376 previous task towards an updated solution for the fluid flow and heat transfer problem.
377 Difficulties at this step come from the fact that Lagrangian trajectories provide updated
378 viscosity values at a number of positions which are irregularly distributed along the Eulerian
379 frame. The Delaunay triangulation was retained as strategy. The application of constraints
380 relying successive positions along a same trajectory proves useful. As a result, the suspension
381 viscosity values available at Lagrangian positions are successfully interpolated into a
382 suspension viscosity field needed at the nodes constituting the Eulerian frame.

383 Before the following iteration, a new Eulerian modeling of fluid flow and heat
384 transfer is performed. It provides updated fields for the velocity, shear rate and temperature.
385 Because this modeling step is performed by taking into account an improved suspension

386 viscosity field, it is expected that these velocity, shear rate and temperature fields represent a
387 somewhat better picture of the fluid flow and heat transfer conditions under the occurrence of
388 product transformation.

389 The coupled problem is solved by iterating the successive Lagrangian and Eulerian
390 steps up to a selected level of convergence. The solution is assumed to be reached when
391 successive viscosity fields exhibit a maximum difference smaller than 0.25 %.

392 This algorithm was implemented through a main program and a set of functions
393 developed in the programming language MATLAB. Eulerian modeling of fluid flow and heat
394 transfer was solved with the help of the COMSOL Multiphysics 3.5a simulation package,
395 using the UMFPAK solver. The implementation of both tasks, including the adoption of
396 other mathematical solvers, seems feasible in other programming languages.

397

398 **3.3. One-dimensional model**

399

400 The transformation of liquid food product under heat treatment has been often
401 represented in the literature by considering average temperature evolution along the
402 exchanger and by assuming plug flow. In this case, both the velocity and temperature fields
403 are assumed to be independent on the distance from the heating wall (e.g., Grijsperdt et al.
404 (2004)). Such an one-dimensional (1D) model is included in the present study for the sake of
405 comparison with a more elaborate approach, in which no assumptions are performed
406 regarding the velocity and temperature fields.

407 Coherently with the application of the Eulerian-Lagrangian approach, the evaluation
408 of the thermal denaturation-aggregation of beta-lactoglobulin requires the unfolding rate
409 constant, (eq. 2) and the aggregation kernel (eq. 6), whose computation asks for local
410 estimates of temperature and shear rate. In the scope of the 1D model, bulk values are used.

411 Assuming that the liquid food product is exposed to an uniform heat flux density Q
 412 (W.m^{-2}), the heat balance for a tubular exchanger can be expressed as:

413

$$414 \quad \rho \bar{v} \pi R^2 C_p d\bar{T} = 2\pi R Q dz \quad (15)$$

415

416 where ρ (kg.m^{-3}) is the product density, \bar{v} (m.s^{-1}) the plug-flow velocity, R (m) the radius of
 417 the exchanger, C_p the specific heat capacity ($\text{J.kg}^{-1}.\text{K}^{-1}$) and \bar{T} (K) the bulk temperature.

418 The integration of equation (15) provides the bulk temperature as a function of the
 419 distance from the exchanger inlet:

420

$$421 \quad \bar{T}\{z\} = T_{inlet} + \frac{Q}{2 \rho \bar{v} R C_p} z \quad (16)$$

422

423 A first-order estimate of the shear rate bulk value required for evaluating particle
 424 aggregation in the 1D model may be obtained from the parabolic flow profile. At a given
 425 radial distance r from the axis of symmetry of the tubular exchanger, the shear rate associated
 426 with parabolic flow can be expressed as:

427

$$428 \quad \dot{\gamma}\{r\} = \frac{4\bar{v}}{R^2} r \quad (17)$$

429

430 Its bulk value is therefore given by:

431

$$432 \quad \bar{\dot{\gamma}} = \frac{\int \dot{\gamma}\{r\} v\{r\} dS}{\int v\{r\} dS} = \frac{32 \bar{v}}{15 R} \quad (18)$$

433

434 Taking into account the geometry and boundary conditions defined above ($R = 5 \text{ mm}$ and \bar{v}
 435 $= 0.0354 \text{ m.s}^{-1}$), we obtain $\bar{\dot{\gamma}} = 15.1 \text{ s}^{-1}$.

436 After estimating bulk values for both the temperature and the shear rate, the
 437 evaluation of the thermal denaturation-aggregation of beta-lactoglobulin can hence be
 438 performed by employing bulk values for both the temperature and the shear rate. For
 439 instance, equation (1) can be rewritten as:

440

$$441 \quad \frac{DC_{nat}\{t\}}{Dt} = \bar{v}\{z\} \frac{dC_{nat}\{z\}}{dt} = -k_n\{z\} C_{nat}^n\{z\} \quad (19)$$

442

443 4. Results

444

445 4.1. Fluid flow and temperature

446

447 Figure 6 shows the velocity, temperature, suspension viscosity and shear rate fields
 448 resulting from the simulations described above.

449 The velocity field (Figure 6a) is assumed as a fully developed flow (parabolic profile)
 450 at the domain inlet. The velocity at the exchanger axis (top of domain) firstly slightly
 451 decreases along the first 30 % of the tube length, and then increases up to the outlet where it
 452 reaches higher values than at the inlet. Near the heating wall, fluid parcels move slower.
 453 Moreover, the region associated with relatively low velocities is broader near the outlet than
 454 at the inlet.

455 Figure 6b shows that temperatures increase along the domain as a consequence of the
 456 developing thermal boundary layer from the heating wall towards the exchanger center.

457 Figure 6c shows that the suspension viscosity increases near the heating wall along
458 the domain, reaching values many times higher near the outlet than that observed at the inlet;
459 moreover, the region associated with increasing suspension viscosity becomes progressively
460 broader along the domain. The latter result is consistent with the decrease of the axial
461 velocity near the heating wall (see Figure 6a).

462 At the domain inlet, the shear rate is proportional to the distance from the exchanger
463 axis as a consequence of the fully-developed incoming flow. However, the shear rate field
464 displayed on the Figure 6d denotes 3 regions: weak values near the exchanger center, b) low
465 values at the wall after an initial increase, and c) between these two patterns, progressively
466 increasing values in a ridge-like region that appears after about 20 % of the exchanger length
467 from the inlet. The first feature is consistent with the symmetry of the velocity profile at the
468 exchanger axis, while the second feature is consistent with the weak velocities occurring in
469 the region near the wall which becomes broader along the domain. The ridge-like pattern
470 with higher shear rates is a consequence of previous features.

471

472 **4.2. Product transformation along trajectories**

473

474 The evolution of the product properties will be analysed along Lagrangian trajectories
475 associated with fluid parcels released at the domain inlet. Each fluid parcel can be considered
476 as a suspension droplet containing an ensemble of whey protein particles at similar
477 thermodynamic and kinetic conditions.

478 Figure 6a displays the five trajectories hereafter taken into account, each of them
479 associated with a given radial release positions at the domain inlet (r_0). These distances were
480 chosen in order to sample different regions of the domain: firstly the exchanger axis, where
481 the highest velocity as well as the minimum transformation are expected ($r_0 = 0$); then the

482 average radial position ($r_0 = 2.5$ mm); and finally three release positions progressively closer
483 to the heating wall ($r_0 = 4, 4.5,$ and 4.75 mm).

484 Figure 7a presents the temperature evolution along these five trajectories, the
485 residence time values from 13.8 up to 174 seconds are indicated on the right. Fluid parcels
486 move slower as they run closer to the wall, being therefore more exposed to heating.
487 Coherently, outlet temperatures increase with r_0 .

488 The evolution of shear rate along these trajectories is displayed in Figure 6b. The
489 shear rate is null on the axis and presents maximum values for the fluid parcels which are
490 moving in the vicinity of the heating wall. The behavior of the two trajectories closest to the
491 wall ($r_0 = 4.5$ and 4.75 mm) indicates first an increase, and then a decrease towards the outlet.
492 The maximum values are associated with the ridge-like feature appearing in Figure 6d. Fluid
493 parcels released near the middle of the domain ($r_0 = 2.5$ and 4 mm) are associated with
494 simpler shear rate evolutions as they do not enter in the ridge-like region.

495 Temperature drives the unfolding kinetics (eqs. 1-2), and drives together with the
496 shear rate the aggregation by modifying the aggregation kernel (eq. 6). As shown in Figure 7,
497 these two key variables exhibit different evolutions along the domain from a trajectory to
498 another. One can therefore expect different unfolding/aggregation histories along the domain
499 under consideration, implying different whey protein particle size distributions at the outlet.

500 Figure 8 presents the evolution of the unfolding ratio -- that is the percentage of
501 proteins that have been unfolded; the volume fraction associated with whey protein
502 aggregates (Φ) and the Sauter mean diameter ($d_{3,2}$).

503 The liquid food product transformation is negligible for fluid parcels moving on the
504 axis ($r_0 = 0$ mm) as well as for those released at the average radial position ($r_0 = 2.5$ mm).
505 This is a consequence of the negligible whey protein unfolding because of the relatively low
506 temperatures experienced along these two trajectories (see Figure 7a).

507 On the other hand, fluid parcels moving in the vicinity of the heating wall ($r_0 = 4.75$
508 mm) experience almost complete unfolding after about 80% of the exchanger length as
509 displayed on Figure 8a. Such a high level of product transformation results from the fast
510 temperature increase over 70 °C. For $r_0 = 4.75$ mm, shear rate is also relatively high along the
511 first 60 % of the trajectory as depicted on Figure 7b; these conditions provide favorable
512 conditions to aggregation. This results in a large increase of the Sauter diameter (Figure 8b)
513 and of the volume fraction of the aggregates. The solid volume fraction increases up to 40 %
514 and the Sauter diameter becomes more than 2000 times larger than its value at the inlet.
515 Intermediate behaviors are exhibited by trajectories associated with fluid parcels released
516 between $r_0 = 2.5$ and 4.75 mm.

517

518 4.3. Viscosity evolution

519

520 The suspension viscosity is driven by the continuous phase (pure water) viscosity as
521 well as by the volume fraction of particles in suspension. Figure 9 shows that the suspension
522 viscosity can appreciably vary along the domain; moreover it can be very different from a
523 given trajectory to another.

524 Fluid parcels moving at the exchanger axis ($r_0 = 0$) and those released at the average
525 radial position ($r_0 = 2.5$ mm) are associated with negligible product transformation (see
526 Figure 8). The suspension viscosity decreases along these trajectories, indicating the role of
527 increasing temperature on the continuous phase viscosity.

528 On the other hand, fluid parcels moving closer to the heating wall ($r_0 = 4.5$ and 4.75
529 mm) experience both a meaningful heating and a high level of product transformation. As a
530 result, the suspension viscosity along these trajectories exhibits a two steps behavior (see
531 Figure 9). On the first half of the exchanger, the suspension viscosity decreases (because

532 continuous phase viscosity is lower for higher temperatures). Then, the product is
533 transformed and aggregation occurs; it involves the increase of the suspension viscosity
534 because that the influence of the growing aggregates volume fraction overtakes the
535 temperature effect on the continuous phase.

536

537 **4.4. Product properties at the outlet**

538

539 After one meter of exchanger, the output product is subjected to a broad diversity due
540 to the different time-temperature-shear rate histories. Figure 10a displays the cumulative
541 volume distribution of the monomers and aggregates at the domain outlet for five selected
542 trajectories.

543 For the two inner fluid parcels ($r_0 = 0$ and 2.5 mm), the aggregation is negligible, the
544 monomers account for more than 98 % of the total volume. The trajectory starting at $r_0 = 4$
545 mm still contains a large number of monomers, but they account only for 6% of the solid
546 volume.

547 For the fluid parcels starting from $r_0 = 4.5$ and 4.75 mm all the proteins are aggregated
548 (no monomer remains). One can sum up that the closer the trajectory is to the heating wall,
549 the higher is the median diameter.

550 Figure 10b displays the particle size distribution of the output bulk product. The
551 output product described using the 2-D Eulerian-Lagrangian model is a blend of the different
552 fluid parcels which a sample is displayed on Figure 10a. Consequently, a large number of
553 monomers averagely remains, they account for 14 % of the solid volume The bulk median
554 radius value is about 1 μm with broad particle size distribution: 20 % of the solid volume is
555 constituted by particles smaller than 0.2 μm and 30 % by particles larger than 5 μm .

556

557 **4.5. Comparison with 1D model results**

558

559 We have argued in the Introduction and shown previously that thermal and dynamic
560 histories can affect the transformation state of the liquid food product.

561 Table 2 presents the product properties at the outlet for both the 2D and the 1D model.
562 The first line displays the ranges of values assumed by selected variables at the domain outlet
563 (r varying from 0 up to $R = 5$ mm), as provided by our 2D simulations. Such ranges are very
564 large, clearly putting in evidence the variety of dynamic and thermal histories experienced by
565 fluid parcels.

566 The following lines in Table 2 present the bulk properties of the output product, that is
567 the properties of the fluid obtained by mixing all the outcoming fluid parcels. These values
568 are those of industrial process interest.

569 Bulk values are far from those associated with fluid parcels released at the average
570 radial position, as shown in the third line of Table 2. This 'average' trajectory ($r_0 = 2.5$ mm) is
571 thus not representative for the process.

572 Last line in Table 2 displays corresponding results provided by the 1-D model
573 described above. This model does not represent the variety of conditions experienced by the
574 liquid food product along the exchanger. It provides essentially the same results as those
575 obtained for fluid parcels released at the average radial position ($r_0 = 2.5$ mm). The results are
576 clearly different from the bulk estimated with the more realistic 2D coupled model.

577

578 **5. Conclusion**

579

580 Thermal denaturation of beta-lactoglobulin in a tubular exchanger has been modeled
581 using a 2D Eulerian/Lagrangian numerical scheme. By splitting the fluid flow and heat

582 transfer model from the transformation determination, a realistic population balance model
583 can be used to estimate the proteins aggregation.

584 The results show the diversity of the output product properties depending on the time-
585 temperature-shear rate histories of the different flow parts: in the region near the wall, the
586 product is heavily heated for a long time, resulting in largely modified product; in the axial
587 region, where the temperature is relatively low and the residence time is shorter, the product
588 is weakly modified.

589 The described numerical approach takes into account the diversity of dynamic and
590 thermal histories experienced by fluid parcels along different trajectories in contrary to the
591 approach where the product is considered as a whole. Indeed, comparison with a simple 1D
592 model shows that bulk properties of the outlet product cannot be predicted in this case
593 without a 2D fully coupled approach.

594 The use of the Eulerian/Lagrangian approach allows the implementation of complex
595 transformation models, as often necessary when dealing with food processing modeling,
596 without the need of oversimplification or model rewriting to comply with the CFD solver
597 structure.

598

599 **Acknowledgement**

600

601 The research leading to these results has received funding from the European
602 Community's Seventh Framework Program (FP7/ 2007-2013) under the grant agreement
603 n°FP7-222 654-DREAM.

604

605 **References**

606

- 607 Abramowitz, M., & Stegun, I.A. (Eds.) (1972). *Handbook of Mathematical Functions, with*
608 *Formulas, Graphs, and Mathematical Tables*. Dover Publications, New York.
- 609 Anema, S.G., & McKenna, A.B. (1996). Reaction kinetics of thermal denaturation of whey
610 proteins in heated reconstituted whole milk. *Journal of Agricultural and Food*
611 *Chemistry, 44*, 422-428.
- 612 Aymard, P., Durand, D., & Nicolai, T. (1996). The effect of temperature and ionic strength
613 on the dimerisation of beta-lactoglobulin. *International Journal of Biological*
614 *Macromolecules, 19*, 213-221.
- 615 Bansal, B., & Chen, X.D. (2006). A critical review of milk fouling in heat exchangers.
616 *Comprehensive Reviews in Food Science and Food Safety, 5*, 27-33.
- 617 Bas, N., Catak, M., Zumaeta, N., Fitzpatrick, J.J., Cronin, K., & Byrne, E.P. (2009).
618 Population balance modelling of protein precipitates exhibiting turbulent flow through
619 a circular pipe. *Chemical Engineering Science, 64*, 4051-4059.
- 620 Batterham, R.J., Hall, J.S., & Barton, G. (1981). Pelletizing kinetics and simulation of full-
621 scale balling circuits. *Preprints of the Third International Symposium on*
622 *Agglomeration*, Nürnberg, Germany.
- 623 Bhole, M.R., Joshi, J.B., & Ramkrishna, D. (2008). CFD simulation of bubble columns
624 incorporating population balance modeling. *Chemical Engineering Science, 63*, 2267-
625 2282.
- 626 Bremer, L.G.B., van Vliet, T., & Walstra, P. (1989). Theoretical and experimental study of
627 the fractal nature of the structure of casein gels. *Journal of the Chemical Society,*
628 *Faraday Transactions, 1, 85*, 3359-3372.
- 629 Byrne, E.P., Fitzpatrick, J.J., Pampel, L.W., & Titchener-Hooker, N.J. (2002). Influence of
630 shear on particle size and fractal dimension of whey protein precipitates: implications

- 631 for scale-up and centrifugal clarification efficiency. *Chemical Engineering Science*,
632 57, 3767-3779.
- 633 De Wit, J.N. (1998). Nutritional and functional characteristics of whey proteins in food
634 products. *Journal of Dairy science*, 81, 597-608.
- 635 De Wit, J.N. (2009). Thermal behaviour of bovine beta-lactoglobulin at temperatures up to
636 150 °C. A Review. *Trends in Food Science and Technology*, 20, 27-34.
- 637 Elofsson, U.M., Dejmek, P., & Paulsson, M.A. (1996). Heat-induced aggregation of beta-
638 lactoglobulin studied by dynamic light scattering. *International Dairy Journal*, 6,
639 343-357.
- 640 Grijspeerdt, K., Hazarika, B., & Vucinic, D. (2003). Application of computational fluid
641 dynamics to model the hydrodynamics of plate heat exchangers for milk processing.
642 *Journal of Food Engineering*, 57, 237-242.
- 643 Grijspeerdt, K., Mortier, L., De Block, J., & Van Renterghem (2004). Applications of
644 modelling to optimise ultra high temperature milk heat exchangers with respect to
645 fouling. *Food Control*, 15, 117-130.
- 646 Hounslow, M. J., Ryall, R. L., Marshall, V. R. (1988). A discretized population balance for
647 nucleation, growth, and aggregation. *American Institute of Chemical Engineers*
648 *Journal*, 34, 1821-1832.
- 649 IAPWS (2008). *Supplementary Release on Properties of Liquid Water at 0.1 MPa*. The
650 International Association for the Properties of Water and Steam, Berlin, Germany.
- 651 Janhoj, T., Petersen, C.B., Frost, M.B., & Ipsen, R. (2006). Sensory and rheological
652 characterization of low-fat stirred yoghurt. *Journal of Texture Studies*, 37, 276-299.
- 653 Kumar, S., Ramkrishna, D. (1996). On the solution of population balance equations by
654 discretization -I. A fixed pivot technique. *Chemical Engineering Science*, 51, 1311-
655 1332.

- 656 Lian, G., Moore, S., & Heeney, L. (2006). Population balance and computational fluid
657 dynamics modelling of ice crystallisation in a scraped surface freezer. *Chemical*
658 *Engineering Science*, *61*, 7819-7826.
- 659 Lyster, R.L.J. (1970). The denaturation of alpha-lactalbumin and beta-lactoglobulin in heated
660 milk. *Journal of Dairy Research*, *37*, 233-243.
- 661 Marchisio, D.L., & Fox, R.O. (2005). Solution of population balance equations using the
662 direct quadrature method of moments. *Journal of Aerosol Science*, *36*, 43-73.
- 663 Navarra, G., Leone, M., & Militello, V. (2007). Thermal aggregation of β -lactoglobulin in
664 presence of metal ions. *Biophysical Chemistry*, *131*, 52-61.
- 665 Norton, T., & Sun, D.-W. (2006). Computational fluid dynamics (CFD) - an effective and
666 efficient design and analysis tool for the food industry: A review. *Trends in Food*
667 *Science & Technology*, *17*, 600-620.
- 668 Péron, N., Heffernan, S.P., Byrne, E.P., Rioual, F., & Fitzpatrick, J.J. (2007).
669 Characterization of the fragmentation of protein aggregates in suspension subjected to
670 flow. *Chemical Engineering Science*, *62*, 6440-6450.
- 671 Sawyer, L., & Kontopidis, G. (2000). The core lipocalin, bovine beta-lactoglobulin.
672 *Biochimica et Biophysica Acta (BBA) - Protein Structure and Molecular Enzymology*,
673 *1482*, 136-148.
- 674 Smoluchowski, M. (1917). Versuch einer mathematischen theorie der koagulationskinetik
675 kolloider lösungen. *Zeitschrift für Physikalische Chemie*, *92*, 129-168.
- 676 Swaisgood, H.E. (1995). Protein and amino acid composition of bovine milk. in *Handbook of*
677 *Milk Composition* (R. G. Jensen, Ed.; Academic Press), pp.464-468.
- 678 Thomas, D.G. (1965). Transport characteristics of suspension: VIII. A note on the viscosity
679 of Newtonian suspensions of uniform spherical particles. *Journal of Colloid Science*,
680 *20*, 267-277.

- 681 Tolkach, A., & Kulozik, U. (2007). Reaction kinetic pathway of reversible and irreversible
682 thermal denaturation of beta-lactoglobulin. *Lait*, 87, 301-315.
- 683 Torres, I.C., Janhoj, T., Mikkelsen, B.O., Ipsen, R. (2011). Effect of microparticulated whey
684 protein with varying content of denaturated protein on the rheological and sensory
685 characteristics of low-fat yoghurt. *International Dairy Journal*, 21, 645-655.
- 686 Verheul, M., Roefs, S.P.F.M., Mellema, J., & de Kruif, K.G. (1998). Power Law Behavior of
687 Structural Properties of Protein Gels. *Langmuir*, 14, 2263-2268.
- 688 Wang, L., & Sun, D.-W. (2006). Heat and mass transfer in thermal food processing, In D.-W.
689 Sun (Ed.), *Thermal Food Processing: New Technologies and Quality Issues* (pp. 35-
690 71). Boca Raton: CRC press.
- 691 Wu, H., Xie, & J., Morbidelli, M. (2005). Kinetics of cold-set diffusion-limited aggregations
692 of denatured whey protein isolate colloids. *Biomacromolecules*, 6, 3189-3197.
- 693 Zumaeta, N., Byrne, E.P., & Fitzpatrick, J.J. (2007). Predicting precipitate breakage during
694 turbulent flow through different flow geometries. *Colloids and Surfaces A:
695 Physicochemical and Engineering Aspects*, 292, 251-263.

696

697 **List of tables**

698

699 Table 1: Chemical kinetics parameters from Anema and McKenna (1996).

700

701 Table 2: Selected variables at the domain outlet.

	T [°C]	$k_{1,5}$ [(mol.m ⁻³) ^{-0.5} .s ⁻¹]
β-lactoglobulin A	70	4.40 10 ⁻⁴
	75	2.31 10 ⁻³
	80	1.08 10 ⁻²
	85	2.68 10 ⁻²
β-lactoglobulin B	70	3.60 10 ⁻⁴
	75	2.62 10 ⁻³
	80	1.46 10 ⁻²
	85	3.96 10 ⁻²

	Unfolding ratio [%]	Sauter diameter [m]	particle volume fraction [%]	number concentration [part/m ³]
2-D (range)	0 to 100 %	$2.0 \cdot 10^{-9}$ to $8.6 \cdot 10^{-6}$	0.35 to 53.62	$2.41 \cdot 10^{14}$ to $1.053 \cdot 10^{23}$
2-D (bulk)	14.1	$1.5 \cdot 10^{-8}$	2.35	$9.05 \cdot 10^{22}$
2-D ($r_0 = 2.5$ mm)	0.1	$2.0 \cdot 10^{-9}$	0.35	$1.052 \cdot 10^{23}$
1-D model	0.7	$2.1 \cdot 10^{-9}$	0.36	$1.046 \cdot 10^{23}$

1 **List of figures**

2

3 Figure 1: Evolution of a suspension of beta-lactoglobulin under continuous heat treatment. (a)

4 simple 1D approach; (b) coupled 2 D approach.

5

6 Figure 2: Numerical domain and boundary condition.

7

8 Figure 3: Pivots representation.

9

10 Figure 4: Particles repartition along pivots after aggregation.

11

12 Figure 5: Iterative procedure.

13

14 Figure 6: Velocity (a), temperature (b), viscosity (c), and shear rate (d) fields on the domain.

15 Domain inlet and outlet are on the left and right respectively, and the heating wall is on the

16 bottom. Five trajectories associated with fluid parcels released at the domain inlet are

17 illustrated with the axial velocity field (a).

18

19 Figure 7: Evolution of temperature (a) and shear rate (b) along fluid parcels trajectories.

20

21 Figure 8: Evolution of unfolding ratio (a), Sauter diameter (b), and aggregate volume fraction

22 (c) along the fluid parcels trajectories.

23

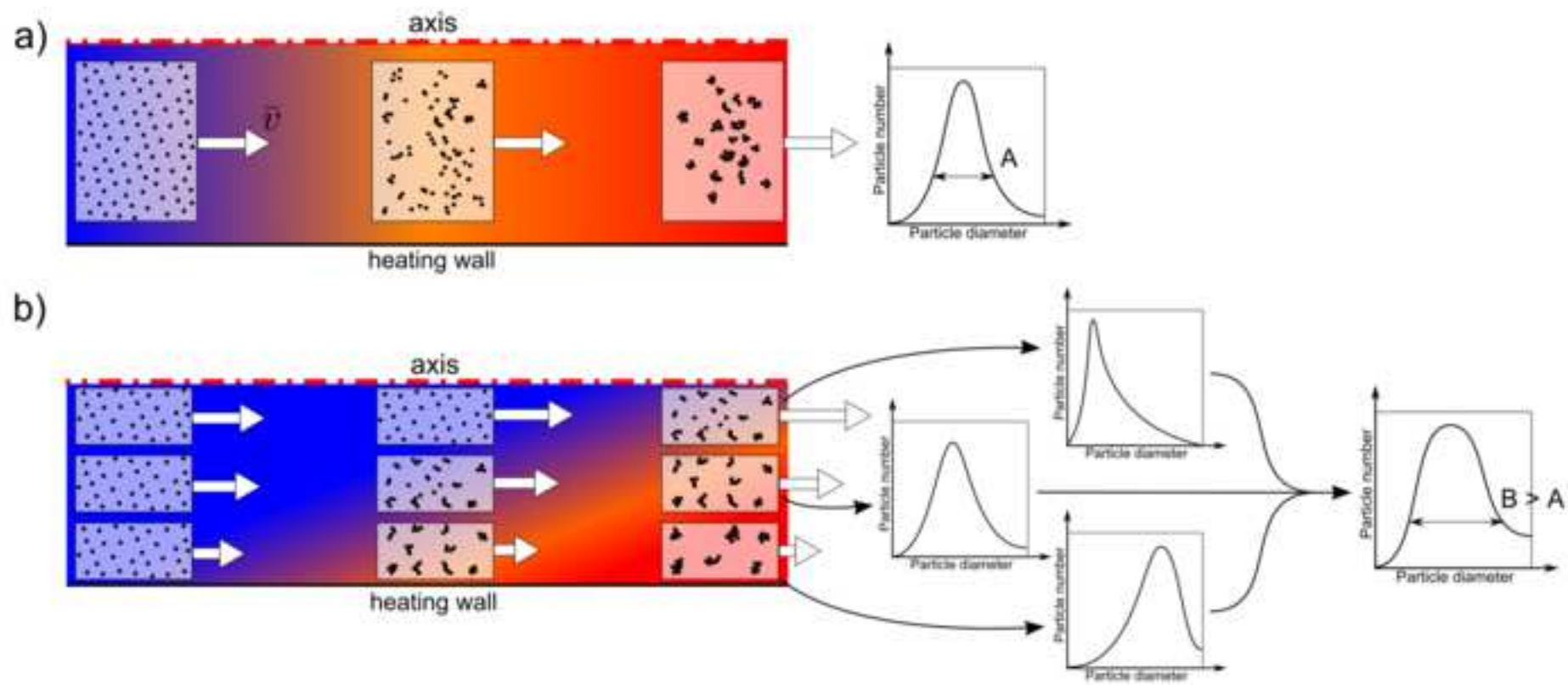
24 Figure 9: Evolution of suspension viscosity along the fluid parcel trajectories.

25

- 26 Figure 10: Cumulative volume distribution of monomers and aggregates at the outlet for: a)
27 five selected trajectories, b) bulk product.

ACCEPTED MANUSCRIPT

Figure 1



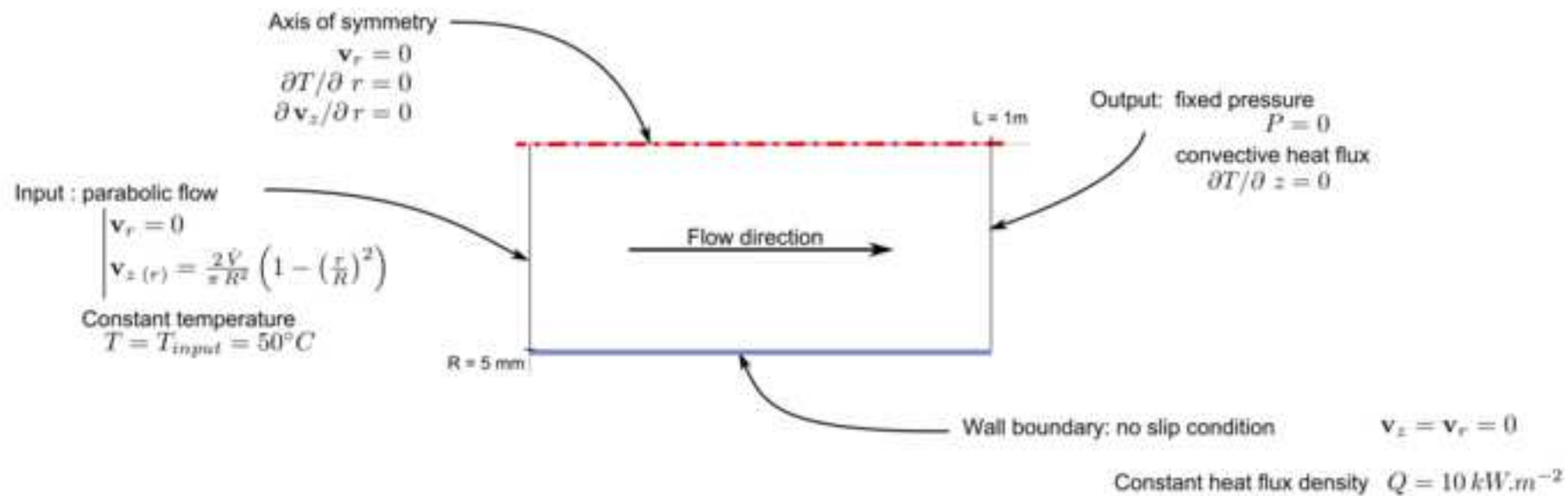


Figure3

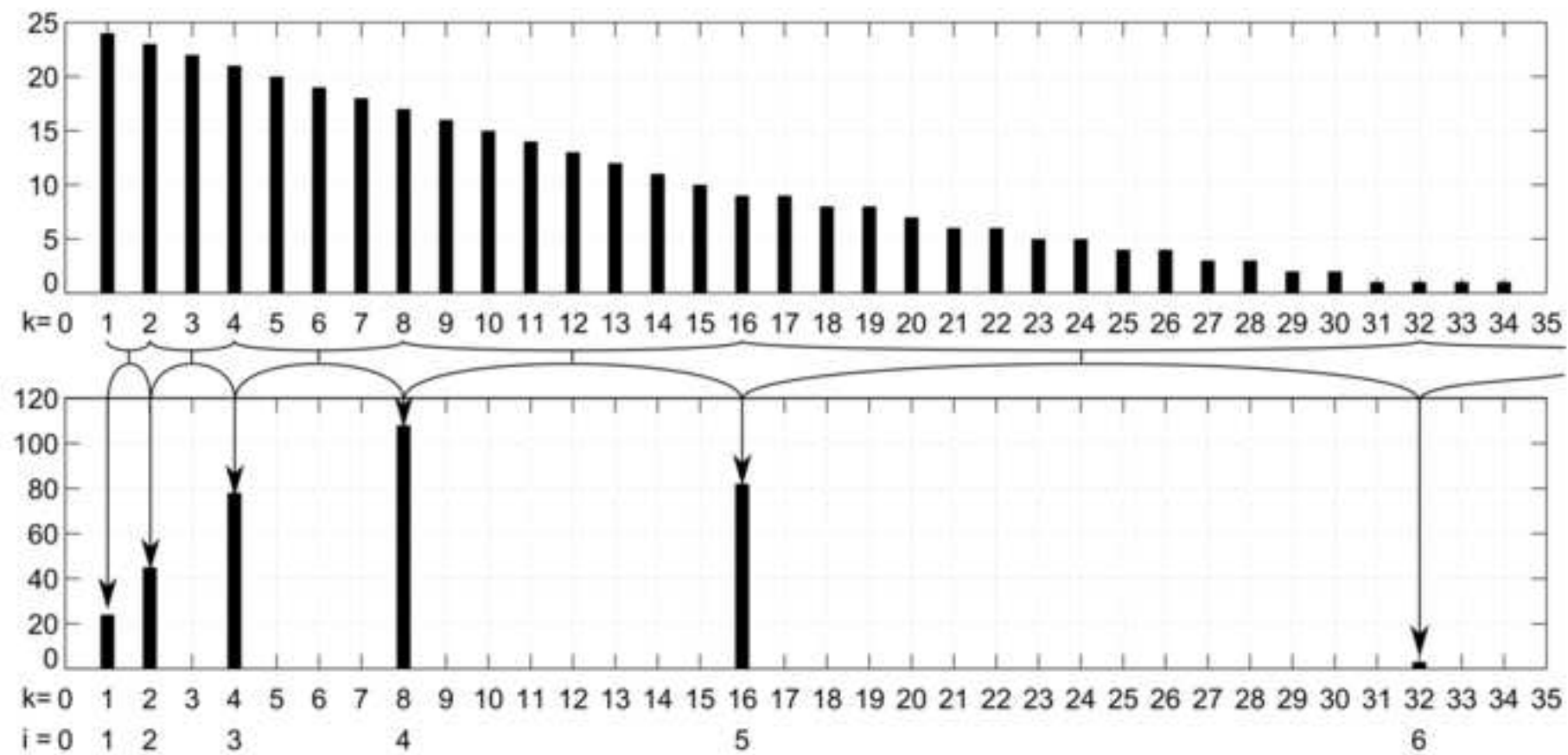
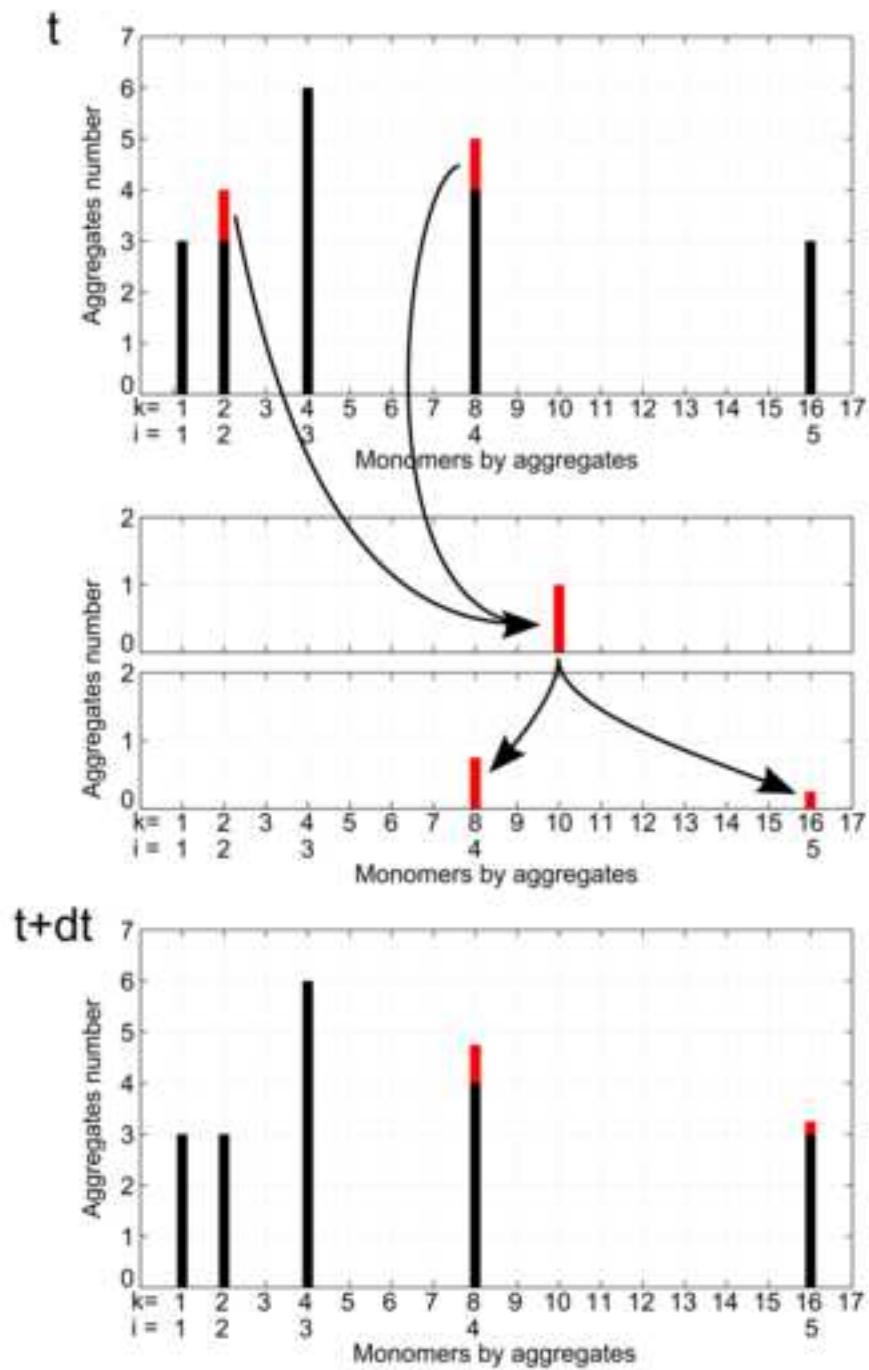
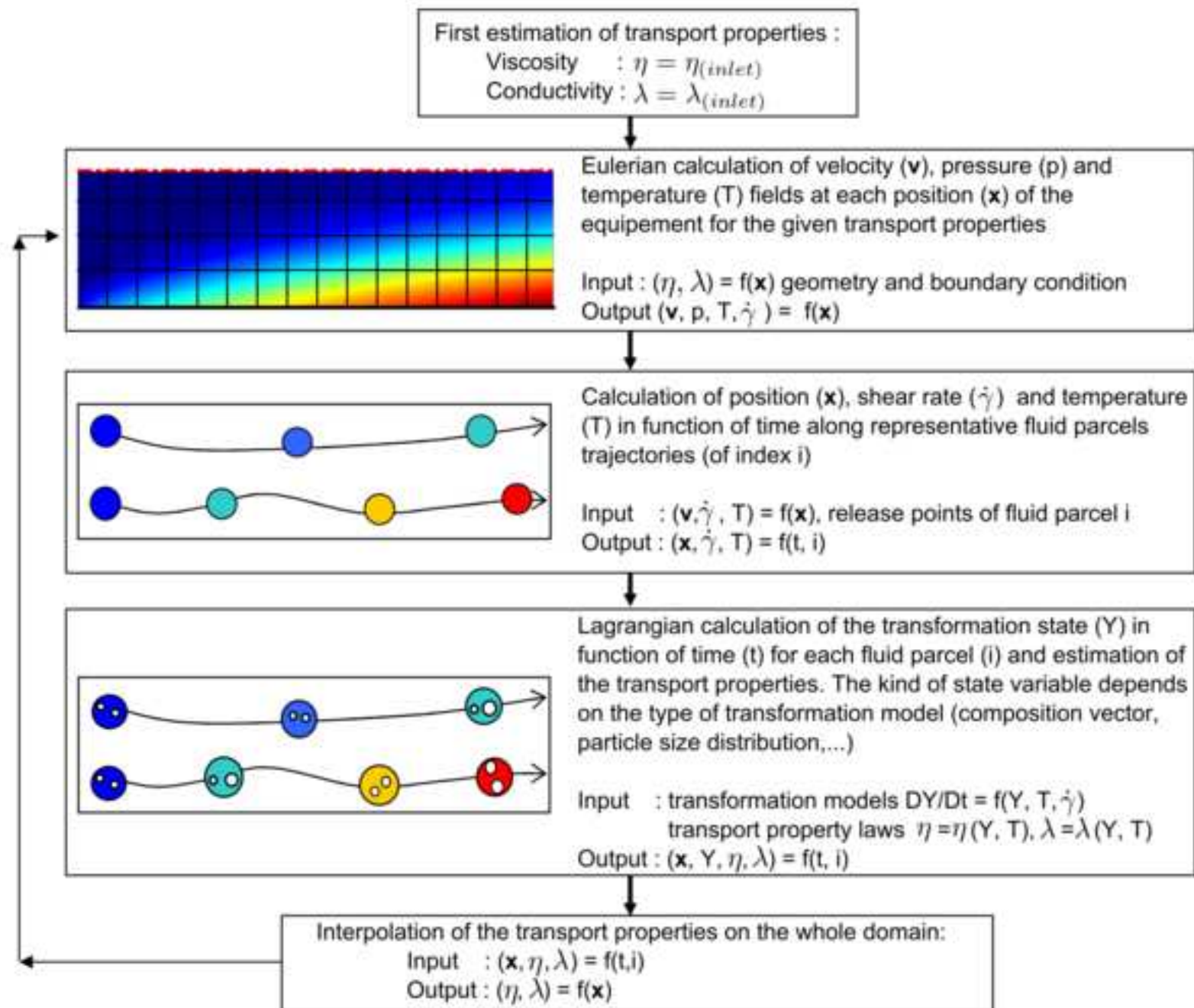
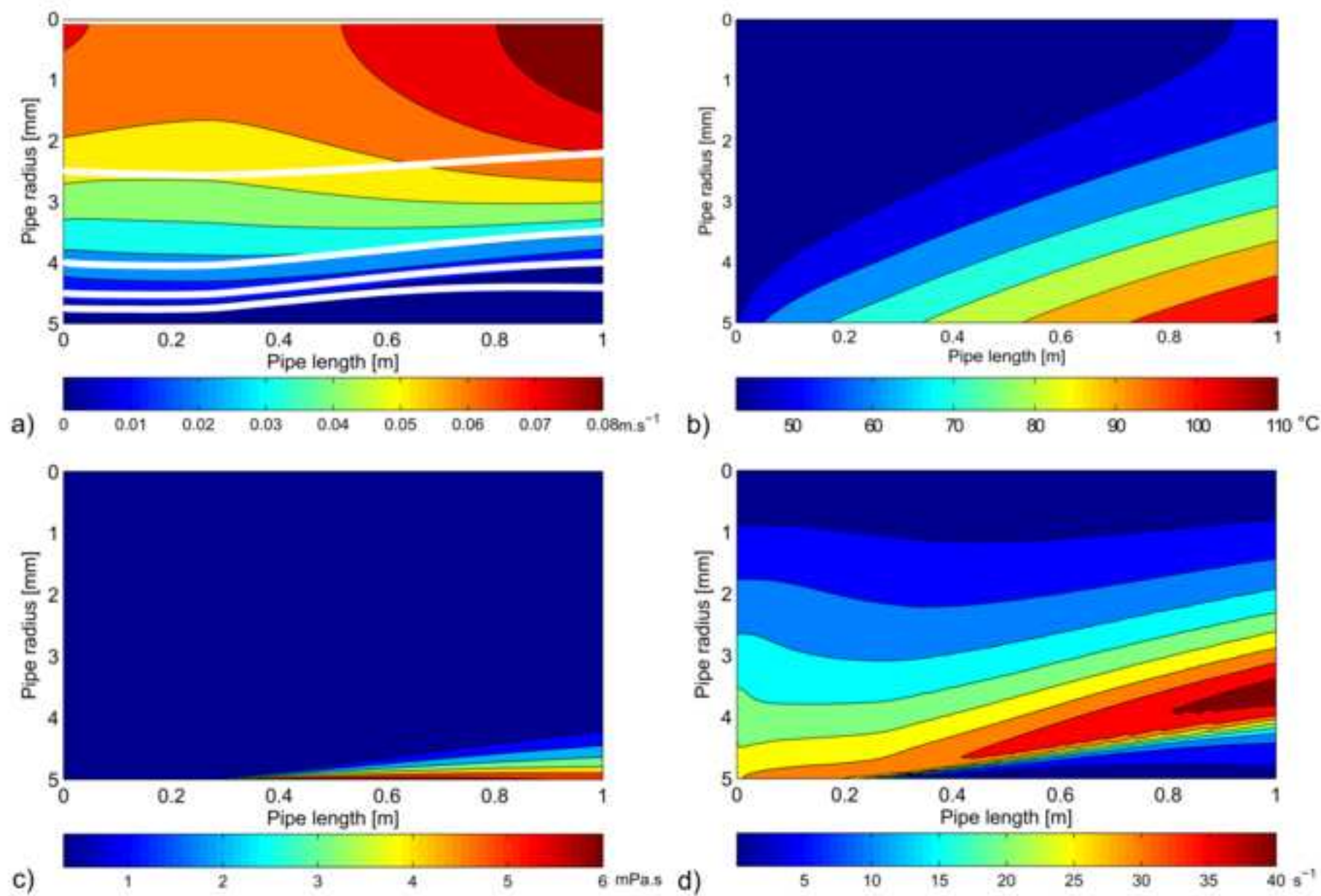
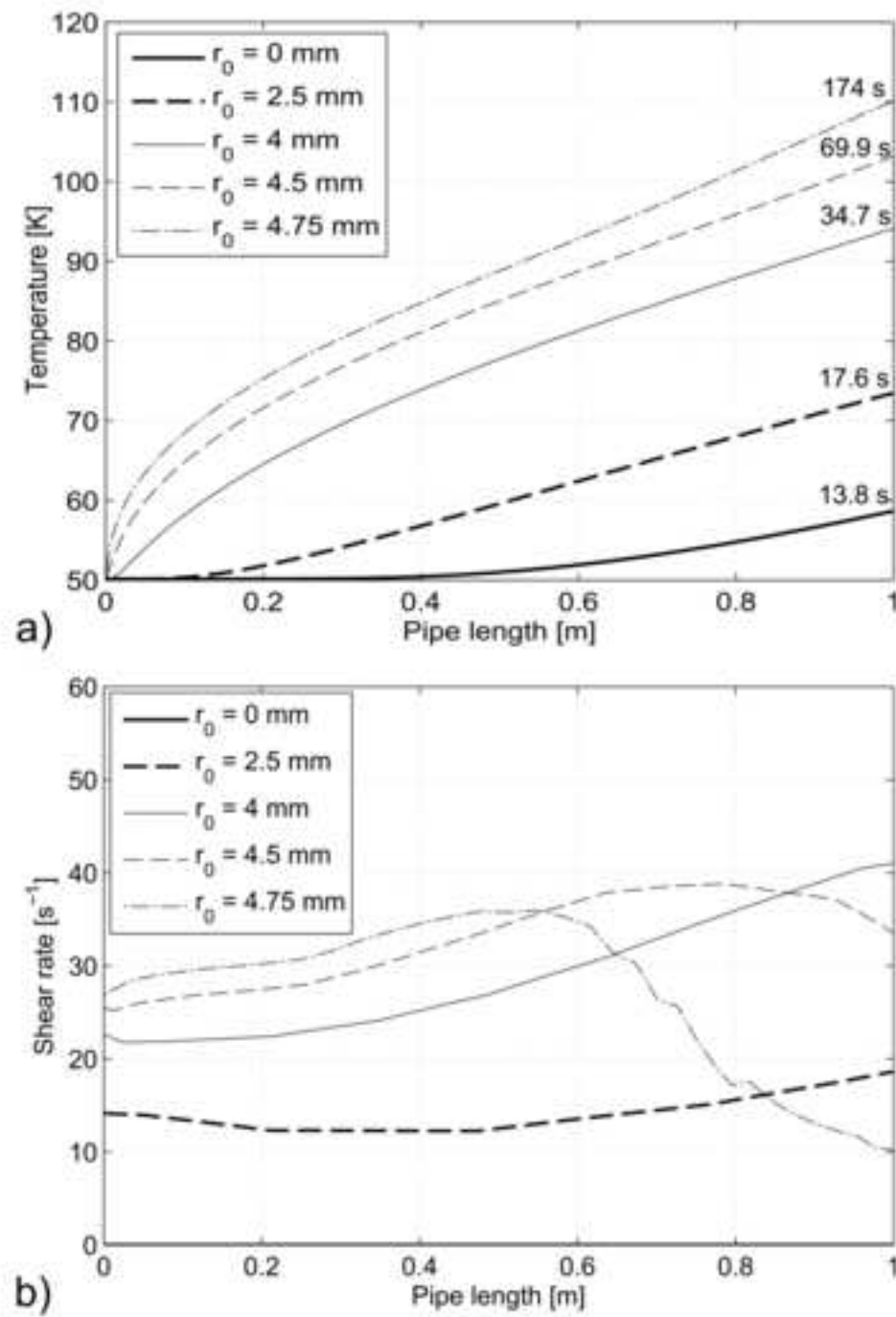


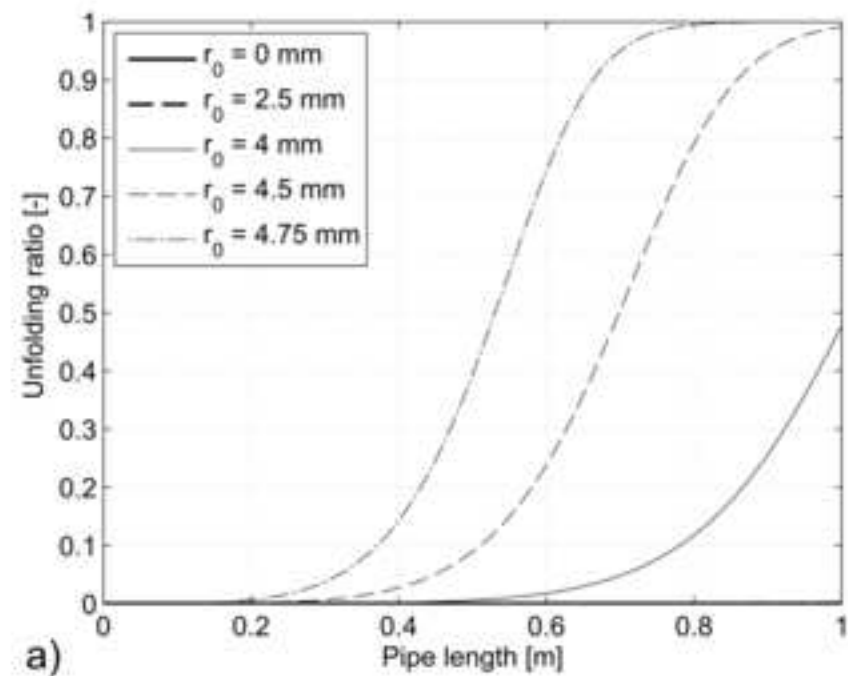
Figure 4



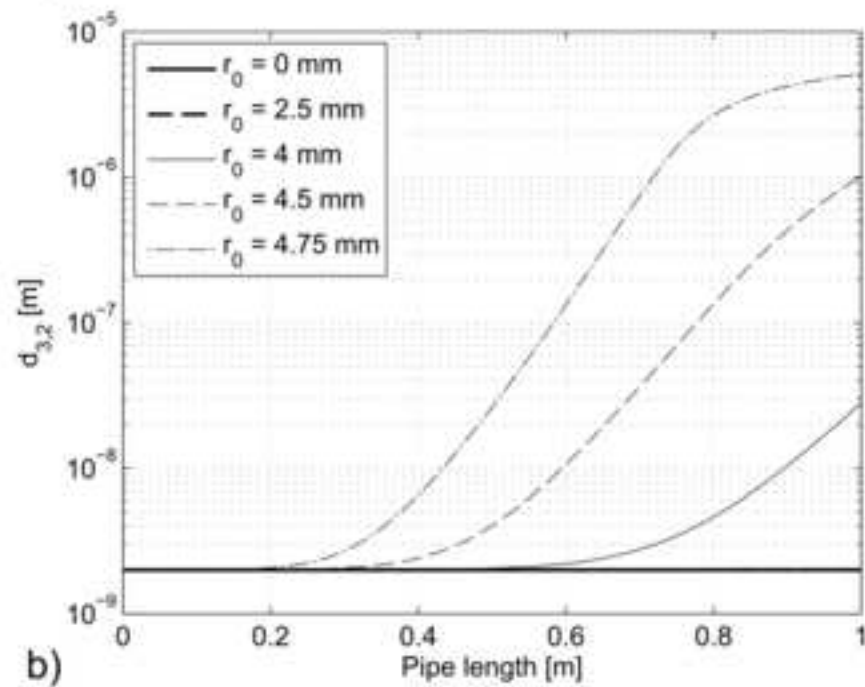




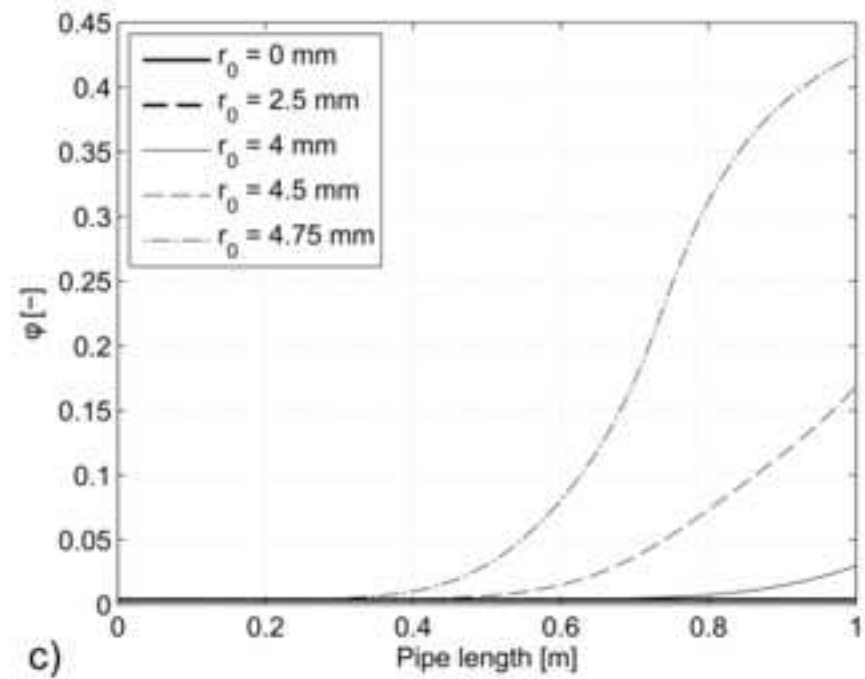




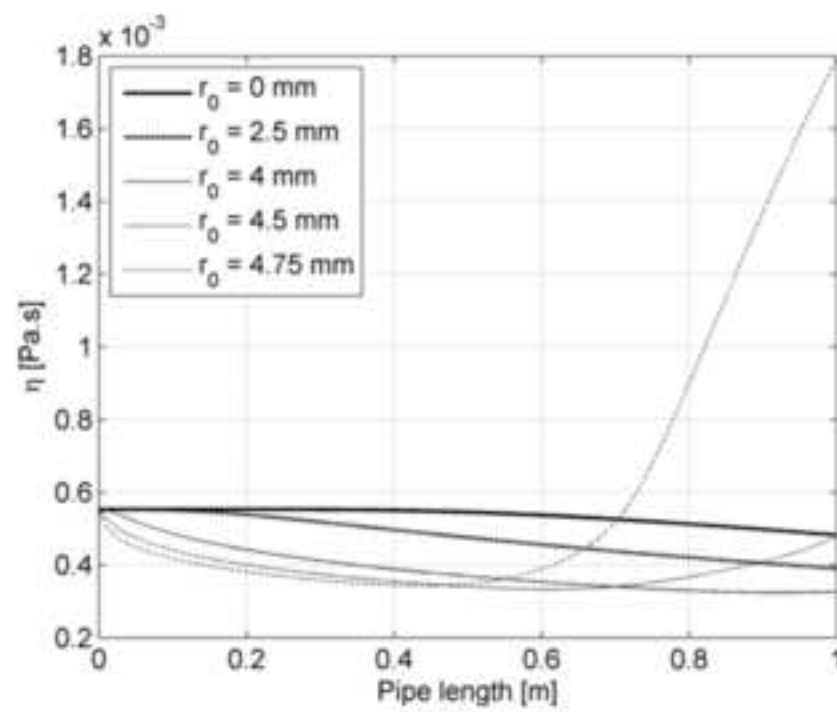
a)

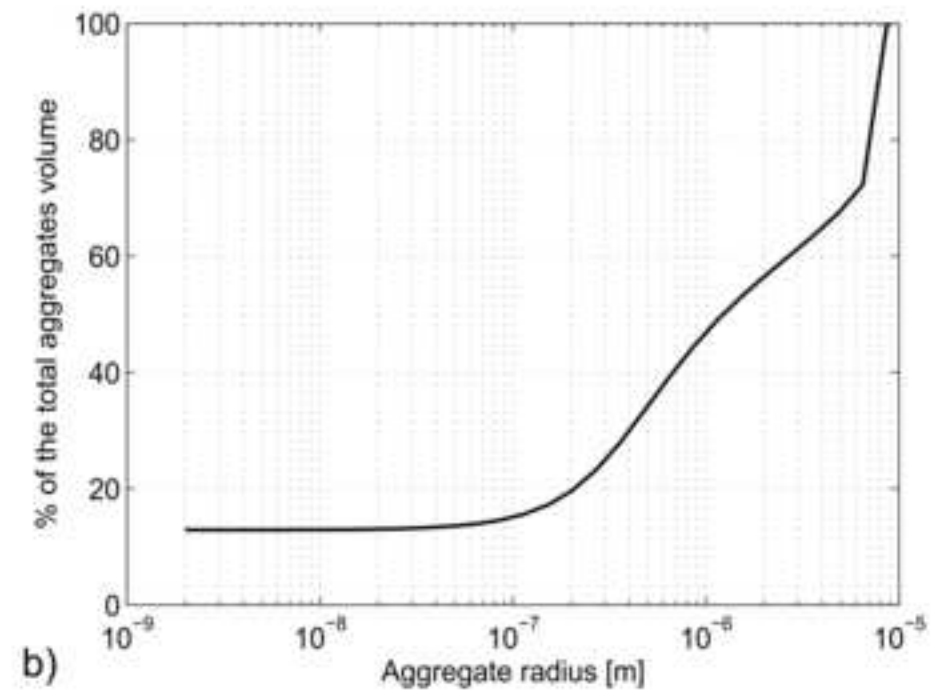
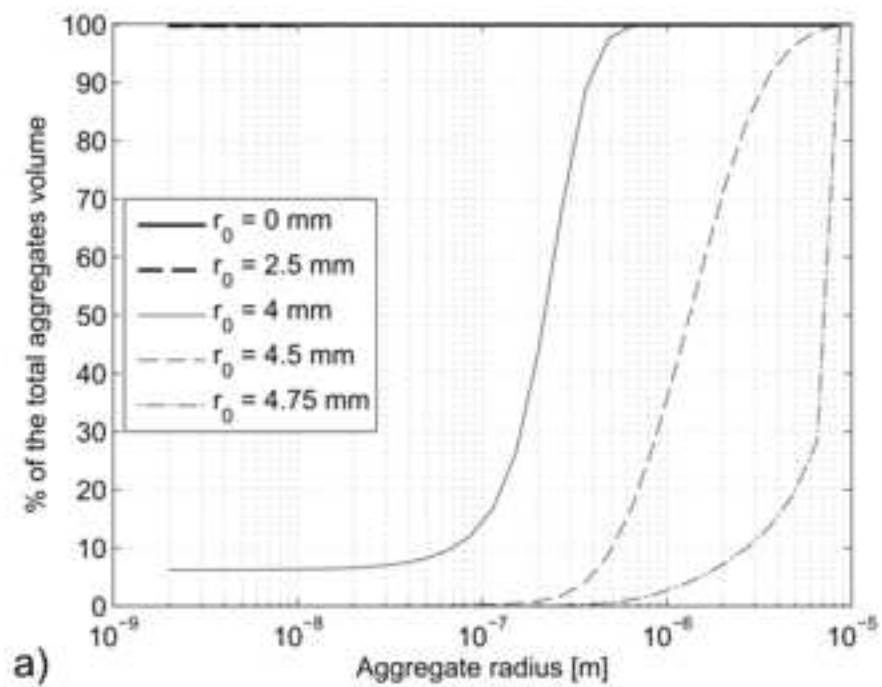


b)



c)





- We study β -lactoglobulin aggregation during continuous thermal treatment.
- Aggregation is estimated along Lagrangian trajectories using sizes class method.
- Transformation is coupled with fluid flow and heat transfer classically estimated.
- Thermal and shear rate histories along the domain drive the aggregation magnitude.
- Obtained particle sizes distribution shows product diversity unlike 1D model.

ACCEPTED MANUSCRIPT

Elsevier Editorial System(tm) for Journal of Food Engineering
Manuscript Draft

Manuscript Number: JFOODENG-D-11-01030R4

Title: Coupling fluid flow, heat transfer and thermal denaturation-aggregation of beta-lactoglobulin using an Eulerian/Lagrangian approach

Article Type: Research Article

Keywords: beta-lactoglobulin; thermal treatment; particle aggregation; population balance equation; computational fluid dynamics; Euler-Lagrange method

Corresponding Author: Dr Artemio Plana-Fattori,

Corresponding Author's Institution: AgroParisTech

First Author: Etienne Chantoiseau

Order of Authors: Etienne Chantoiseau; Artemio Plana-Fattori; Christophe Doursat; Denis Flick

Abstract: The transformation of liquid food product under heat treatment is often represented by considering average temperature evolution along the exchanger and by assuming plug-flow. Our aim is to demonstrate that thermal denaturation-aggregation of whey proteins can be more realistically represented by taking into account the different dynamical and thermal histories associated with fluid parcels which progress more or less quickly, far or close to the heating wall, inside the processing unit. A numerical approach is proposed for evaluating the thermal denaturation-aggregation of whey proteins, combining computational fluid dynamics and the population balance equation. The approach is illustrated by the evolution of a suspension of beta-lactoglobulin. Fluid flow and heat transfer are solved through the finite element method in the Eulerian frame, while product transformation is evaluated along representative Lagrangian trajectories. Outlet bulk results show that the product reaches a higher level of transformation than in assuming plug-flow and radially-independent temperature.